An Interdecadal Oscillation in an Idealized Ocean Basin Forced by Constant Heat Flux

RICHARD J. GREATBATCH AND SHENG ZHANG

Department of Physics, Memorial University of Newfoundland, St. John's, Newfoundland, Canada

(Manuscript received 11 November 1993, in final form 17 March 1994)

ABSTRACT

The authors report on a regular, interdecadal oscillation in a three-dimensional ocean circulation model. The model is run using box geometry of size comparable to the North Atlantic and is driven by a constant, zonally uniform, surface heat flux. The meridional overturning in the model exhibits a peak to peak oscillation of 7 Sv about a mean of 15 Sv. The period is 50 years. The oscillation has many similarities to that found by Delworth et al. in the GFDL coupled ocean–atmosphere model. In particular, the SST anomaly pattern during the oscillation is quite similar to that in the coupled model and also to interdecadal anomaly patterns seen in SST data from the North Atlantic. Since the surface flux is constant, the oscillation is due to a balance between convergence in the oscillating part of the poleward heat transport and changes in local heat storage. A similar balance applies to the coupled model where changes in surface heat flux weakly oppose the oscillation. Including salinity, by adding a zonally uniform surface salt flux forcing, acts to weaken the oscillation but does not change its form. This is also consistent with the coupled model. The oscillation is also found when the surface heat flux is calculated interactively, by coupling the ocean model to a zero-heat-capacity model of the atmosphere. The authors suggest that an oscillation of this kind may have played a role in the warming of the North Atlantic surface waters during the 1920s and 1930s and the subsequent cooling in the 1960s.

1. Introduction

Recent results from the Geophysical Fluid Dynamics Laboratory (GFDL) coupled ocean–atmosphere model (Delworth et al. 1993) have shown the existence of an irregular oscillation in the thermohaline circulation in the North Atlantic with a timescale of 40–50 years. The irregular oscillation appears to be driven by density anomalies in the sinking region of the thermohaline circulation, combined with much smaller density anomalies of opposite sign in the broad, rising region. Figure 1, taken from Delworth et al. (1993), shows that changes in the surface buoyancy flux play only a weak role in the oscillation, with the changes in the surface heat flux acting to oppose the contribution from poleward heat transport but with the latter dominating the total. The oscillation, therefore, appears to be a mainly oceanic event. Indeed, Fig. 1 suggests that it should be possible to produce a similar oscillation in an ocean-only model driven by constant surface flux fields. This forms the mandate of the present paper.

There is growing evidence to indicate the importance of decadal variability in the climate system. Ghil and Vautard (1991) have noted the importance of removing the decadal signal from globally averaged surface air temperatures if we are to properly access the rate of global warming. The North Atlantic seems to be of particular importance and has attracted the most attention [see Gordon et al. (1992) for a review]. The possible role of changes in the thermohaline circulation and the associated poleward heat transport was first raised by Bjerknes (1964) and is further discussed by Bryan and Stouffer (1991). Kushnir (1994) has presented evidence to support the view that sea surface temperature (SST) variations in the North Atlantic with a 30–40-year timescale are influenced by changes in the ocean circulation. Delworth et al. (1993) pointed out the similarity between the SST anomaly pattern associated with the 40–50-year oscillation in the coupled model and the pattern of North Atlantic SST variability found by Kushnir (1994), lending support to the coupled model results. Further evidence for the role of the ocean circulation has been provided by Deser and Blackmon (1993). These authors suggest that the general warming in North Atlantic SST during the 1920s–1930s, followed by a cooling in the 1960s, may have been associated with changes in the Gulf Stream. In particular, they point to the decrease in Gulf Stream transport in the early 1970s, compared to the late 1950s, implied by the diagnostic calculations of Greatbatch et al. (1991) and supported by the work of Sato and Rossby (1993). There is also evidence that the subsurface structure of the North Atlantic exhibits decadal variability. For example, by comparing composites for the pentads 1955–59 and 1970–74, Levitus (1989a,b,c) found that potential density surfaces within the core of the subtropical gyre were as much as 50 m

Corresponding author address: Dr. Richard J. Greatbatch, Department of Physics, Memorial University, St. John's, Newfoundland A1B 3X7, Canada.

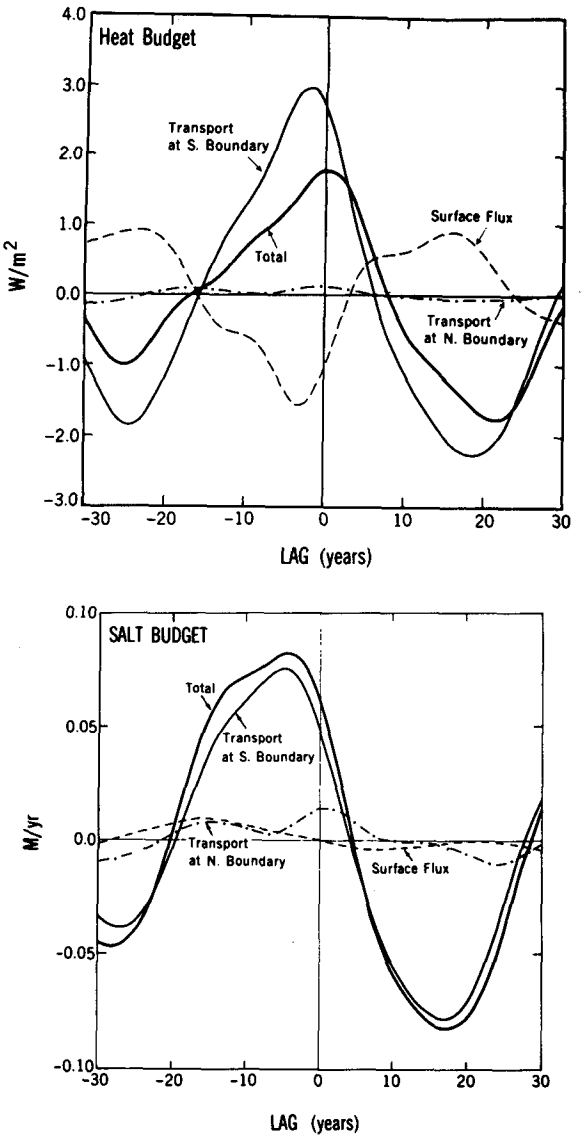

FIG. 1. The heat and salt budgets for the sinking region of the North Atlantic thermohaline circulation in the GFDL coupled model [taken from Delworth et al. (1993)]. Values greater than zero imply a net flux into the sinking region. The details of the regression analysis used to obtain these plots can be found in Delworth et al.

higher in the later pentad and up to 100 m lower in the northern recirculation region (Hogg et al. 1986) to the north of the Gulf Stream. Greatbatch and Xu (1993) have shown that at 24°N the poleward heat transport associated with these changes is reduced in the 1970–74 pentad compared to climatology, although it is not clear if such a reduction actually occurred. Read and Gould (1992) have traced subsurface changes in the thermohaline structure of the North Atlantic. They relate these changes to the cessation of deep-water formation in the Labrador Sea in the late 1960s and early 1970s (Lazier 1980). This was associated with the "Great Salinity Anomaly" (Dickson et al. 1988) and the capping of the waters in the Labrador Sea by unusually fresh water.

Following Marotzke (1990) and Weaver and Sarachik (1991a,b), decadal and interdecadal oscillations have been reported in a number of ocean-only models run under mixed boundary conditions (that is, the use of a restoring boundary condition on the surface temperature and a flux boundary condition on the surface salinity). Examples are provided by Winton and Sarachik (1993), Weaver et al. (1993), and the coarse-resolution North Atlantic model of Weaver et al. (1994). Decadal oscillations have also been found in models due to the coupling between the ocean and sea ice (Yang and Neelin 1993; Zhang et al. 1994). Decadal timescale oscillations under a constant flux condition have previously been reported by Huang and Chou (1994) in the context of the haline circulation with no heat flux forcing and an overturning circulation with deep water formed at low latitudes. Huang and Chou did conduct one additional experiment in which they reversed the sign of the freshwater flux forcing, leading to an overturning circulation with sinking at high latitudes. In this experiment, they found an oscillation similar to that we shall present here. However, they made no attempt to relate their work to that of Delworth et al. (1993) or the data studies of Kushnir (1994) and Deser and Blackmon (1993), preferring instead to emphasize the use of a flux boundary condition as a model for the freshwater flux forcing of the ocean.

The plan of this paper is as follows. Section 2 briefly describes the ocean model. Section 3 presents the model results. Section 4 provides a summary and discussion.

2. The numerical model

The model used is the planetary geostrophic ocean general circulation model described by Zhang et al. (1992). It is a generalization to many levels of Killworth's (1985) two-level model. The governing equations consist of the full prognostic temperature and salinity equations and diagnostic momentum equations. The latter consist of the geostrophic balance and a linear friction in the vertically averaged part in order to provide a western boundary current. The equation of state is quadratic in temperature and linear in salinity and is given by

$$\rho(T, S) = 3.0 + 0.77S - 0.072T(1 + 0.072T). \quad (1)$$

Here T is temperature in degrees Celsius, S is salinity in practical salinity units, and ρ is (density $-$ 1000) in units of kilograms per cubic meter. The coefficients are similar to those of Bryan and Cox (1972) but with compressibility effects ignored. The convective overturning algorithm ensures a completely stable profile after mixing (Marotzke 1991). The full model equa-

tions, their physical justification, and the model verification can be found in Zhang et al. (1992).

The model uses spherical coordinates. For this study, the model domain consists of a flat-bottomed, 60° square box in latitude–longitude space extending between 5° and 65°N. The horizontal resolution is the same as in Zhang et al. (1993): that is, 2° in both latitude and longitude. Fourteen levels are used in the vertical. Table 1 gives the depth at the center of each level. The total depth of the model ocean is 4000 m. There is no wind stress applied. The model was initialized with a state of rest and uniform values for the temperature and salinity of 3.5°C and 33 practical salinity unit (psu), respectively. The model was then spun up using a specified surface heat flux, shown in Fig. 2, that is zonally uniform and is kept constant throughout the integration. The salt flux was set to zero so that the salinity maintains the constant value of 33 psu. [Runs including salt flux forcing are described in section 3. Note that the ocean sees a freshwater flux. Here, this is modeled as a "virtual" salt flux, as described by Huang (1993).] The vertical and horizontal diffusivity used in the temperature T and salinity S equations have uniform values of 1.00×10^{-4} m^2 s^{-1} and 1.5×10^3 m^2 s^{-1}, respectively. The mean state, averaged over the last 1000 years of integration, is shown in Fig. 3. Throughout this averaging period, the model exhibits no drift. The zonally averaged temperature and the SST fields are quite realistic in appearance and exhibit a reasonable range between the tropical and polar latitudes. The average magnitude of the overturning circulation is 15 10^6 m^3 s^{-1} (Sv), with deep water being formed at high latitudes.

3. Model results

The solid line in Fig. 4 shows the time series of the overturning streamfunction. (The dashed line is for the case with salinity to be discussed later in this section.) After some initial adjustment, the model settles down into a regular oscillation about a mean value of 15 Sv. The period is near 50 years, and the peak-to-peak amplitude is about 7 Sv. The oscillation persists in the same regular fashion throughout a further 2000 years of integration.

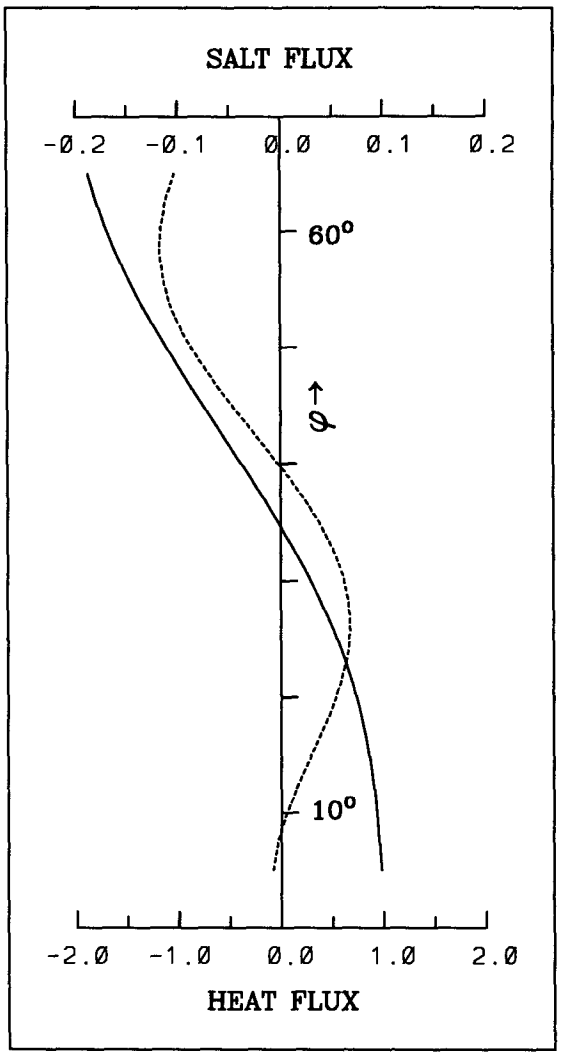

FIG. 2. The solid line shows the zonally uniform heat flux used to drive the model. The units are °C per month for the 46-m top model level. The dashed line shows the zonally uniform salt flux used in the second experiment. The units are psu per month for the 46-m top model level.

TABLE 1. The depths of the center of each model level.

Layer number	Depth (m)
1	23
2	75
3	140
4	223
5	327
6	458
7	623
8	831
9	1093
10	1423
11	1838
12	2362
13	2990
14	3664

Figure 5 shows anomalies (that is, with the mean removed) of zonally averaged temperature and meridional overturning at 12.5-year intervals (1/4 of the oscillation period). The second and fourth rows are at the time when the overturning streamfunction reaches its maximum and minimum values, respectively. The corresponding anomalies for the SST and surface velocity are shown in Fig. 6. SST anomalies of up to 2°C can be seen. These appear to rotate in a counterclockwise direction about a "center of action" near the western boundary at 55°N. Similar behavior is exhibited

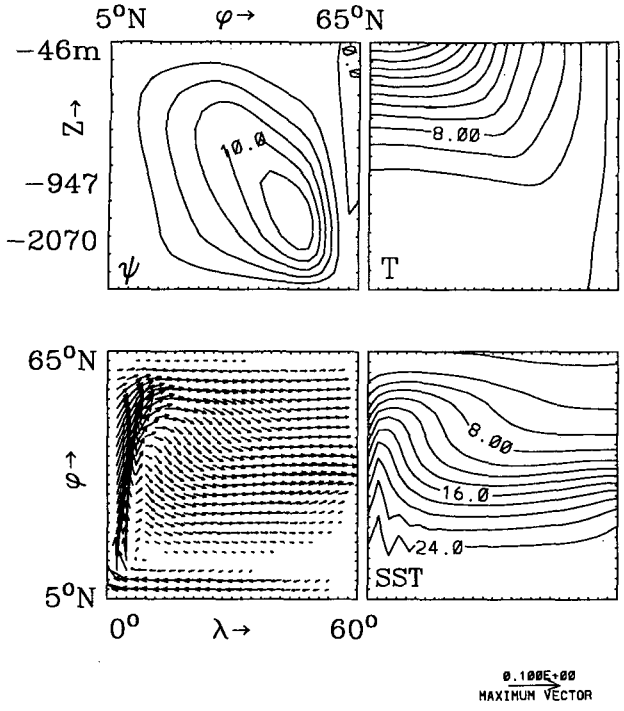

FIG. 3. The mean state, showing the overturning streamfunction ψ, zonally averaged temperature T, SST, and the surface velocity field. The contour intervals are 2.5 Sv and 2°C, respectively, and the smallest arrow length corresponds to a velocity of 0.005 m s^{-1}. In the upper two panels, the vertical scale is that of the model levels, the depths of which are given in Table 1. This means that the figure is distorted in the vertical direction, with the upper part expanded.

by the SST anomalies in the GFDL coupled model (T. Delworth 1993, personal communication) and also by the anomalies of dynamic topography (surface to 915 m) computed by Delworth et al. (1993). Indeed, there is a striking similarity between the pattern of our SST anomalies and that of the dynamic topography anomalies shown in Fig. 7. The close similarity between our surface velocity anomalies and the velocity anomalies from the coupled model is also apparent. (Note that whereas our plots extend from 5° to 65°N, Delworth et al.'s extend from 20° to 90°N.) The temperature anomalies seen at the surface in our model extend throughout the depth of the thermocline. This can be seen in Fig. 5 for the case of anomalies in the zonally averaged temperature. Anomalies extending throughout the depth of the thermocline are also a feature of the data study of Levitus (1989a). Similarly, the cooling event at the Panulirus station off Bermuda, noted by Roemmich (1990) and centered around 1970, also extended throughout the upper 1500 m of the water column.

Figure 8 shows SST difference fields computed by Delworth et al. (1993) using output from the coupled model, and by Kushnir (1994) using Comprehensive Ocean–Atmosphere Data Set (COADS) data from the North Atlantic. For comparison, Fig. 9 shows a similar SST difference field from our model. (In this case, the difference is between averages over the 10 years following each of panels b and d in Fig. 6.) There is a general similarity of shape between all three SST difference fields, although the amplitude in our case is somewhat larger. There are probably many reasons for the increased amplitude in our case, one factor being our assumption that the surface heat flux remains constant. (The opposing role played by changes in the surface heat flux was noted in connection with Fig. 1.) Another factor is likely to be the irregular nature of the oscillation in the coupled model (and in the North Atlantic data) compared to the very regular oscillation in our model. In addition, we shall see later in this section that including salinity in our model acts to reduce the magnitude of the oscillation and, hence, the associated SST anomalies.

Comparing the anomalies in the meridional overturning with those of the zonally averaged temperature (Fig. 5), we see that as the overturning becomes stronger than the mean (positive anomaly), the zonally averaged temperature increases in high latitudes. This is associated with the northward movement of the positive SST anomaly as seen in Figs. 6a–c. Then, as the overturning becomes weaker than the mean (Figs. 5d,e), the zonally averaged temperature decreases in high latitudes, with the northward-moving positive SST anomaly now replaced by a northward-moving negative SST anomaly. The mechanism of this oscillation appears to be quite simple. Since the surface heat flux is constant, the temperature anomaly at high latitudes is controlled by the strength of the advection from low latitudes. This means that when the overturning is stronger than the mean, temperatures at high latitudes increase, as we have seen above. On the other hand, the strength of the overturning is itself influenced by the temperature anomaly and can be expected to decrease in response to the increase in temperature at high latitudes. In this way, the enhanced overturning

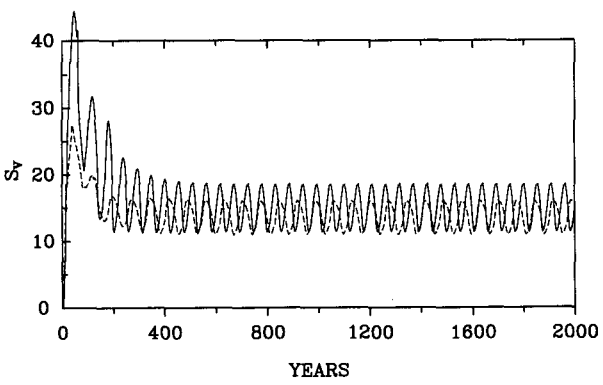

FIG. 4. The maximum value of the overturning streamfunction during the first 2000 years of integration. The solid line is for the case driven by heat flux alone. The dashed line includes salt flux forcing.

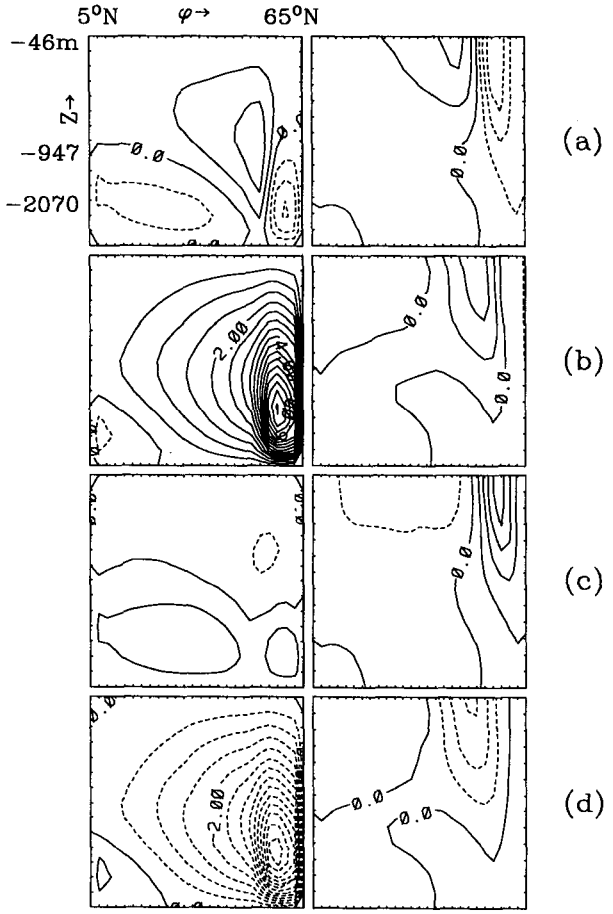

FIG. 5. Anomalies (that is, difference from the mean) of the overturning streamfunction (left column) and the zonally averaged temperatures (right column). Each of (a), (b), (c), and (d) are 12.5 years apart, with the meridional overturning being a maximum at (b) and a minimum at (d). The contour intervals are 0.5 Sv and 0.5°C, respectively. Negative anomalies are shown using dashed contours. As in Fig. 3, the vertical scale is expanded in the upper part of the water column.

contains the seeds of its own decline, and the overturning subsequently weakens and passes into the reverse phase. We can also understand this from another point of view. Since there is a constant rate of heat loss at high latitudes, the surface residence time of a water particle determines the temperature anomaly at high latitudes. When this residence time is short—as when the overturning circulation is stronger than the mean—less heat is removed by the high-latitude cooling and positive temperature anomalies result. Such an anomaly can be seen in Fig. 6b along the path of the separated western boundary current (see Fig. 3) at a time when the surface velocity anomalies in Fig. 6b are enhancing this current. This relatively buoyant water then acts to reduce the strength of the overturning and, subsequently, to increase the surface residence time of water parcels. Water parcels are then cooled more than before, leading to an elimination of the buoyant anomaly and its replacement by relatively dense water (Figs. 5d and 6d) that sinks and acts to enhance the circulation. In this way, the cycle repeats itself.

The above mechanism was put forward by Huang and Chou (1994) as an explanation for the oscillations they found under constant freshwater flux forcing. Huang and Chou also noted that the frequency of the oscillation increased almost linearly with the amplitude of the freshwater flux. The oscillations were also very sensitive to the values of the vertical and horizontal diffusivity and the horizontal grid resolution, sometimes showing a doubling of the period and sometimes chaotic behavior. We have not carried out such a comprehensive sensitivity study here. One problem is that changing the strength of the forcing and the model parameters also changes the structure of the mean state, driving it away from the quasi-realistic state we have in Fig. 3. On the other hand, both the period and amplitude of the oscillation are certainly sensitive to changes in the strength of the forcing, model parameters (see later), and also model resolution. For example, a model using a two-hemisphere version of our 60° box, but only 4° resolution instead of the 2° used here (and correspondingly different model parameters), exhibits a very similar oscillation but with a period of 25 years (Cai et al. 1994).

We have already noted the similarity between our anomaly fields in Figs. 5 and 6 and those from the Delworth et al. (1993) coupled model shown in Fig. 7. Figure 10 shows the different contributions to the

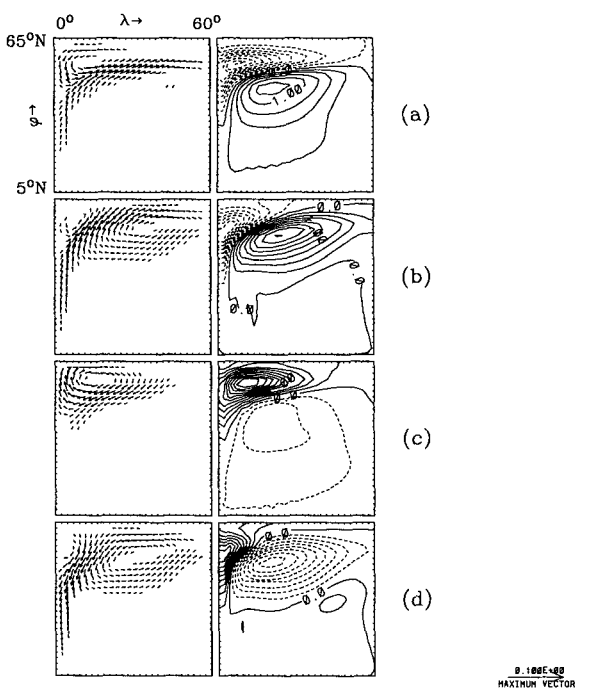

FIG. 6. As Fig. 5 but for the surface velocity and the sea surface temperature. The contour interval is 0.25°C, and the smallest arrow length corresponds to a velocity anomaly of 0.005 m s^{-1}.

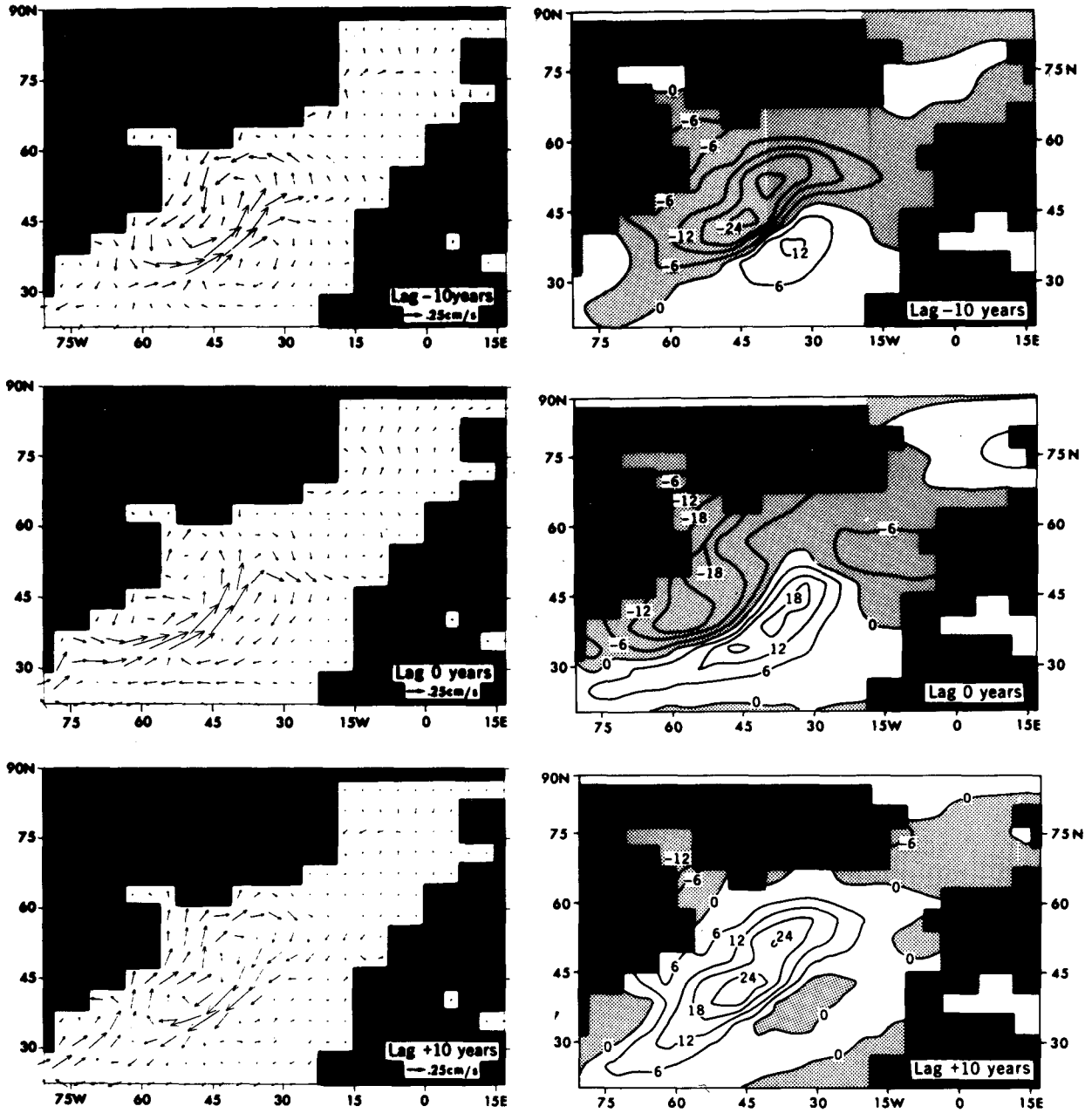

FIG. 7. Anomalies of the velocity at 170-m depth (left-hand column) and of dynamic topography (surface to 915 m) from the GFDL coupled model corresponding to Figs. 6a–c [taken from Delworth et al. (1993)]. The units of dynamic topography are 10^2 cm^2 s^{-2} and values less than zero are stippled. The details of the regression analysis used to obtain these figures can be found in Delworth et al.

dynamic topography anomalies in Fig. 7 from each of the temperature $\Delta D'_T$ and salinity $\Delta D'_S$. We see that the dynamic height contribution due to salinity $\Delta D'_S$ has a similar pattern to that of temperature but has the opposite sign and about 1/3 of the magnitude. Thus, the sign of the dynamic height anomaly in the coupled model (Fig. 7) is determined by the temperature with the salinity acting to reduce the anomaly. This has already been noted by Delworth et al. (1993). These authors claim that the anomalous horizontal circulation set up by the dynamic topography anomalies is important for generating salinity anomalies in the sinking region of their model and that the density in the sinking region is primarily controlled by salinity. They claim this is essential for the oscillation in their model to occur. On the other hand, the oscillation we have described occurs in a model in which the salinity is everywhere uniform, with no freshwater flux forcing

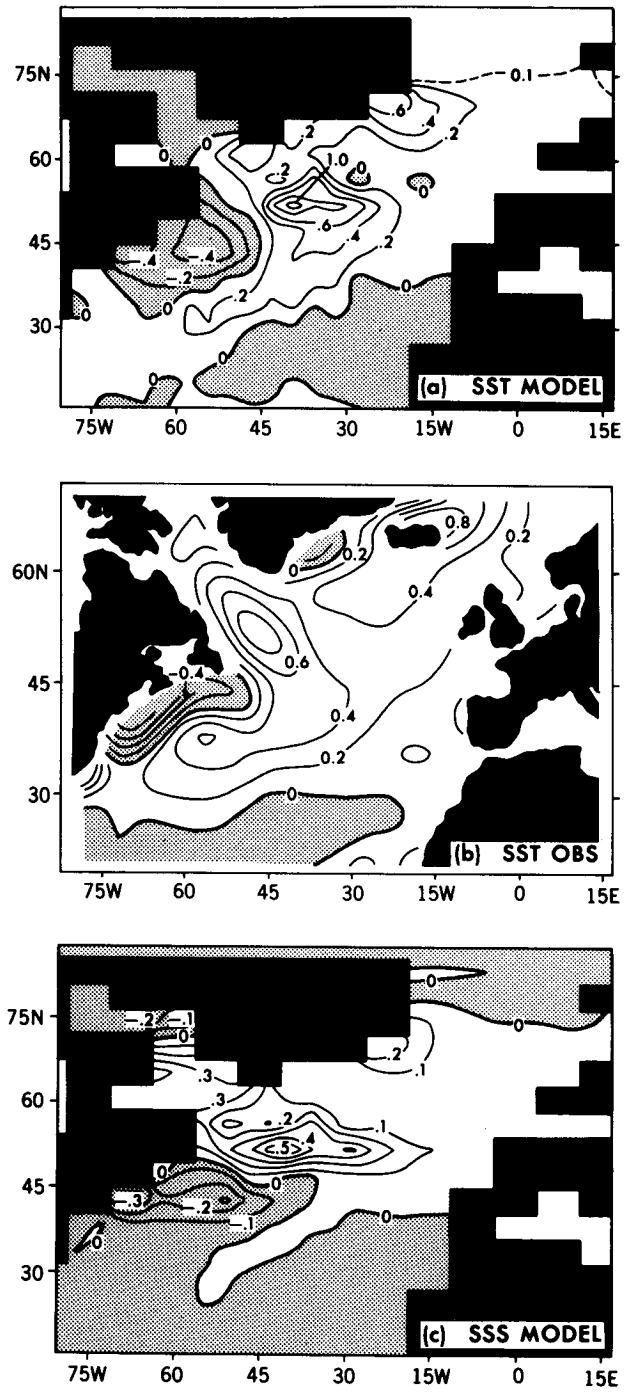

FIG. 8. (a) Differences in annual mean SST from the GFDL coupled model between four decades with anomalously large thermohaline overturning and four decades with anomalously low thermohaline overturning. Units are in °C. Values less than zero are stippled. (b) Differences in observed SST between the periods 1950–1964 (warm period) and 1970–1984 (cold period). Units are in °C. Values less than zero are stippled [adapted from Kushnir (1994)]. (c) As (a) but for sea surface salinity. Units are practical salinity units. From Delworth et al. 1993.

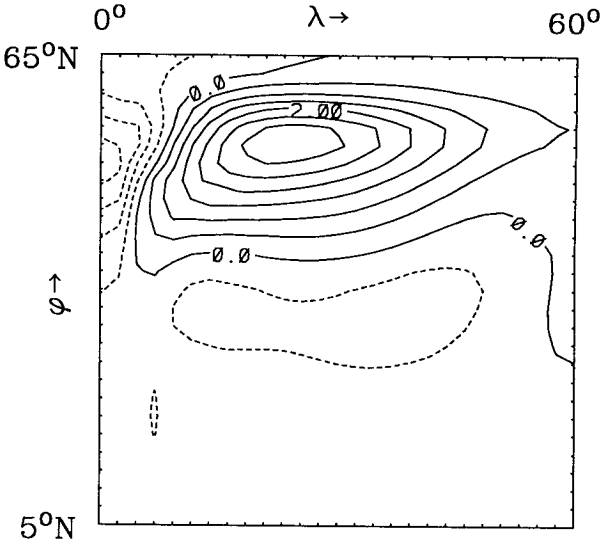

FIG. 9. The difference between the average of the model SST over the 10 years following Fig. 6b, and that over the 10 years following Fig. 6d. The contour interval is 0.5°C. Dashed contours indicate negative values.

at the surface. We suggest instead that the oscillation in the coupled model is entirely thermally driven and that the role of salinity is to act as a brake on the oscillation by opposing the influence of the temperature anomalies on the density.

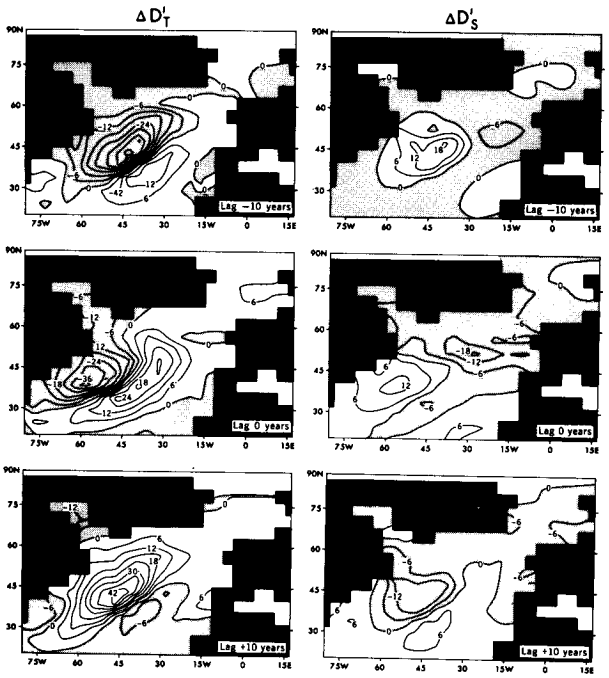

FIG. 10. Decomposition of the dynamic topography anomalies in Fig. 7 into parts associated with temperature $\Delta D'_T$ and salinity $\Delta D'_S$. Units are 10^2 cm^2 s^{-2}, and the contour interval is 6×10^2 cm^2 s^{-2}. (From Delworth et al. 1993).

We now illustrate this by describing an oscillation in a model run that includes forcing by a zonally uniform salt flux. This is given by the dashed line in Fig. 2. In addition, the amplitude of the specified surface heat flux is increased by 6%, and the values of the vertical and horizontal diffusivities are changed to 1.33×10^{-4} m^2 s^{-1} and 1.2×10^3 m^2 s^{-1}, respectively (a slight increase for the vertical diffusivity, slight decrease for the horizontal diffusivity). The model was spun up as before, resulting in a realistic mean state (not shown). Quite strong oscillations occur in the early part of the spin up, but eventually a regular oscillation is established with a period of 70 years (20 years longer than before) and a peak to peak amplitude of 5 Sv. (This is the dashed line in Fig. 4.) Figure 11 shows the anomalies of the surface density together with the contributions from temperature and salinity. The similarity of these anomalies to those of the SST in Fig. 6 is immediately apparent. (Note that the sign of the anomalies for the temperature contribution is opposite to that in Fig. 6. This is because in Fig. 11 we are plotting the density anomaly associated with the temperature rather than the temperature anomaly itself.) We can also see that the salinity contribution opposes that of the temperature and acts to reduce the total density anomaly. This agrees with the interpretation given above that salinity acts to reduce the magnitude of the oscillation. This is not surprising, since now the salinity anomalies generated by the fluctuations in the meridional overturning can be expected to have the opposite effect on the density in high latitudes to that of the temperature anomalies. For example, when the overturning is enhanced compared to the mean, the residence time of water parcels at the surface is reduced. This means that surface water parcels will be cooled less but also freshened less compared to the mean state, leading to a warm, salty anomaly at high latitudes. Clearly, the effect of the salinity anomaly is opposite to that of the temperature anomaly, leading to a reduced density anomaly and a weakened oscillation.

An interesting feature of this experiment is that the anomalies of temperature and salinity are highly correlated at all depths of the model ocean. In particular, regions of anomalously low temperature are also regions of anomalously low salinity, and vice versa, but with the temperature anomaly always dominating and determining the sign of the density anomaly. The same behavior is exhibited by the difference fields of temperature and salinity constructed by Levitus (1989a) using North Atlantic data from the pentads 1955–59 and 1970–74. Indeed, Levitus found a positive correlation between the temperature and salinity differences 1970–74 minus 1955–59 at all depths of the North Atlantic, with correlations exceeding 0.8 throughout the depth range 200–800 m.

We have also conducted additional experiments to check the robustness of the oscillation. Increasing the vertical diffusivity increases the magnitude of the oscillation since there is more potential energy associated with the deeper pycnocline. Decreasing the horizontal diffusivity has the same effect since there is less damping of temperature anomalies in the western boundary current region. The sensitivity of the period to the values of the diffusivities, the strength of the forcing, and the model resolution have already been noted in connection with Huang and Chou's (1994) work. Although periods in the interdecadal range are always found, these can vary considerably from case to case. This indicates that the timescale of oscillations, such as found by Delworth et al. (1993), is probably highly model dependent but that the occurrence of interdecadal variability is a robust feature. We have also found damped oscillations that decay until a steady state is reached. For example, introducing salinity forcing can lead to damping (again consistent with our view that salinity acts to oppose the oscillation). Also, when the forcing is weak, decreasing the vertical diffusivity and increasing the horizontal diffusivity can also lead to damping. Diffusivities appropriate to the ocean are not well known. However, the use of smaller horizontal diffusivities in higher-resolution models may favor the oscillation.

Experiments have also been carried out in which the surface heat flux is calculated interactively by coupling

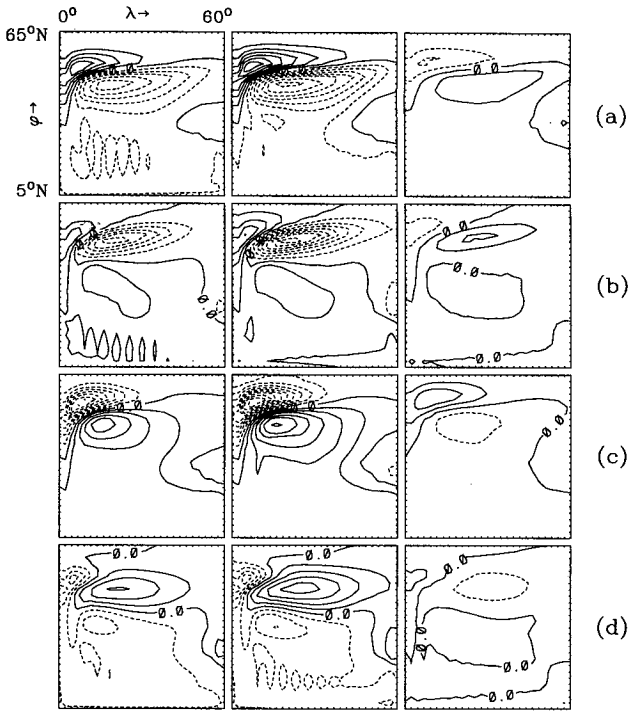

FIG. 11. Anomalies in the surface density (left-hand column) and the contributions from temperature (center column) and salinity (right-hand column) in the experiment with both heat and salt flux forcing. Each of (a), (b), (c), and (d) are 17.5 years apart, with the meridional overturning being a maximum at (b) and a minimum at (d). The contour interval is 0.05 kg m^{-3}.

our ocean model to the zero heat capacity atmosphere model of Schopf (1983). The effect is to restore the surface temperature in the model to a specified temperature T_r on a timescale of several hundred days [see Zhang et al. (1993) for the details]. The temperature T_r corresponds to the radiative equilibrium temperature of the atmosphere in the absence of air–sea heat exchange. Oscillations with the same character as under constant heat flux have again been found [see Cai et al. (1994) for an example]. Changes in the surface heat flux act to weaken the oscillation, as happens in the GFDL coupled model (Fig. 1). This is not surprising. Positive SST anomalies are now associated with anomalous heat loss from the ocean, and negative SST anomalies with anomalous heat gain, in opposition to the changes in local heat storage induced by the variations in the poleward heat transport. Oscillations are also found in cases that include constant salt flux forcing. It should be noted that these oscillations differ fundamentally from oscillations found under mixed boundary conditions (Weaver and Sarachik 1991a,b). Under mixed boundary conditions, the surface temperature is restored to a specified "restoring temperature" on a timescale of tens of days rather than the hundreds of days used here. For this reason, surface temperature never departs far from the restoring temperature. The sign of an anomaly in surface density is then determined by the surface salinity. This contrasts with the oscillations described in this paper, in which the sign of an anomaly in surface density is determined by the surface temperature, as in Fig. 11, even in cases that include salt flux forcing. A detailed comparison between the oscillations found here and oscillations found under mixed boundary conditions will be given in a future manuscript.

Finally, all the experiments in this paper use zonally uniform forcing. It turns out that zonal uniformity is not necessary. A small zonal redistribution of the surface buoyancy flux, diagnosed from a restoring spin up experiment, is enough to induce oscillations, as described in Cai et al. (1994).

4. Summary and discussion

We have reported on a regular oscillation in an ocean model driven by constant heat flux forcing. The period is 50 years and the magnitude is 7 Sv peak to peak in the case of the meridional overturning, about a mean of 15 Sv. We used box model geometry of size comparable to the North Atlantic and have shown that the oscillation has many similarities to that in the Atlantic sector of the GFDL coupled atmosphere–ocean model discussed by Delworth et al. (1993). In particular, the model SST anomaly pattern agrees well with the coupled model and with the North Atlantic data studies of Kushnir (1994) and Deser and Blackmon (1993), despite our use of a simple, zonally uniform, constant, surface heat flux boundary condition. The mechanism is associated with the balance between the strength of the poleward heat transport and local heat storage. This is similar to what is found in the coupled model (Fig. 1), in which the changes in surface heat flux play a weak, opposing role. Delworth et al. emphasized the role played by horizontal advection of salinity in their model. They argue that the thermally dominated dynamic height anomalies in Fig. 7 drive horizontal circulations that change the salinity in the sinking region of their North Atlantic overturning circulation. They claim these changes in salinity drive the oscillation in their model. On the other hand, the oscillation in our model is entirely thermally driven. Indeed, the basic experiment is run with no-salt flux forcing at the surface and a uniform value of salinity. In an experiment that includes salt flux forcing, we find a high correlation between changes in temperature and changes in salinity, with the resulting salinity anomalies acting oppositely on density from the temperature anomalies but with the temperature anomalies determining the sign of the density anomalies. In this way, salinity acts to oppose the oscillation. A similar high correlation between temperature and salinity anomalies, with temperature determining the sign of the density anomaly, has been found by Levitus (1989a) in data from the North Atlantic.

The results reported here use zonally uniform, constant surface flux forcing. The model parameters, forcing, and output fields all exhibit realistic values. We have associated our oscillation with the long timescale (40–50 year) changes in North Atlantic SST noted by Kushnir (1994) and Deser and Blackmon (1993), in particular, the warming during the 1920s and 1930s, followed by a cooling in the 1960s, associated with Deser and Blackmon's EOF 1 shown in Fig. 12. Both papers suggest a role for the ocean circulation in determining these SST changes. Both also note the different nature of the observed variability at shorter interannual to interdecadal timescales. For example, EOF 2 in Fig. 12 exhibits variability at a timescale near 10 years. As noted by Deser and Blackmon, for this EOF, warm SST anomalies are associated with anomalous heat gain by the ocean and cold SST anomalies by anomalous heat loss. This suggests a local mechanism, in which the changes in ocean circulation are unimportant and the SST anomalies are driven by heat flux forcing from the atmosphere. It also contrasts sharply with the heat flux variations found in models run under mixed boundary conditions (e.g., Weaver and Sarachik 1991a). This is because under mixed boundary conditions the use of the restoring boundary condition on the surface temperature leads to enhanced heat loss when the SST is anomalously high and to increased heat gain when SST is anomalously low, in direct contrast to the observed data. Deser and Blackmon (1993) show a connection between decadal variations in sea ice in the Labrador Sea and the SST variations associated with their EOF 2, with periods of greater than

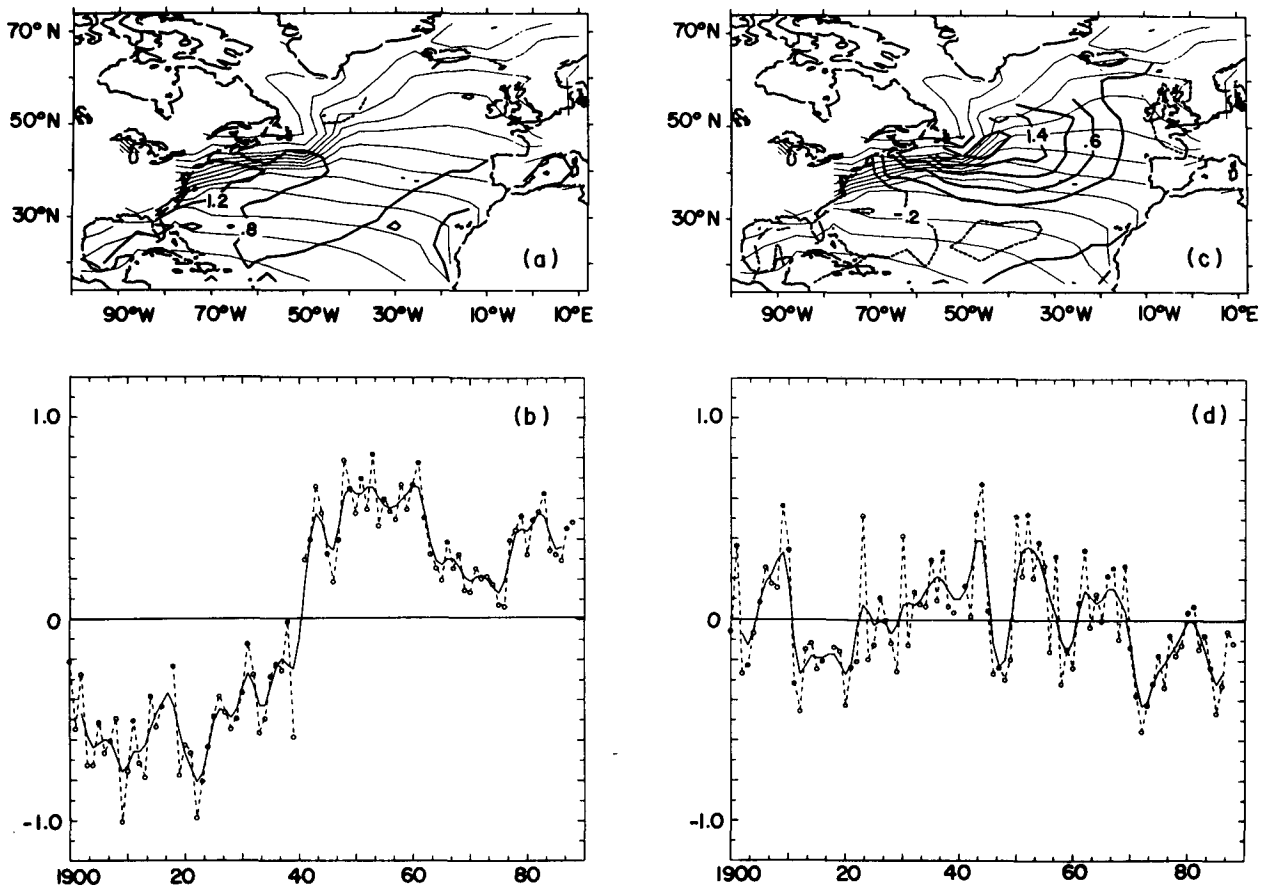

FIG. 12. (a) EOF 1 of North Atlantic SST anomalies based on unnormalized winter (November–March) means 1900–89 (bold contours). Also shown is the climatological SST (thin contours). (b) Time series of EOF 1 (dashed curve) and smoothed with a five-point binomial filter (solid curve). (c) and (d) As in (a) and (b) but for EOF 2 [from Deser and Blackmon (1993)].

normal sea ice extent preceding, by about 2 years, periods of colder than normal SST east of Newfoundland. This suggests a possible role for coupled ice–ocean oscillations, such as described by Zhang et al. (1994), for explaining the behavior exhibited by EOF 2. It should be noted that the oscillation we have described also differs fundamentally from oscillations found in models run under mixed boundary conditions. This is because in our model, changes in the surface density are dominated by changes in the surface temperature (see Fig. 11), whereas under mixed boundary conditions, changes in surface density are controlled by changes in surface salinity. However, in both cases, relatively low surface temperatures are associated with relatively low surface salinities, and vice versa.

One final comment. We have also carried out an experiment in which the model is initialized with the state obtained by time averaging over many oscillation periods (such as shown in Fig. 3). The oscillation always develops within a few hundred years and has the same form and amplitude as before. It seems, therefore, that for some steady, surface flux fields there is no corresponding steady response of the ocean.

Acknowledgments. We are grateful to Tom Delworth, Suki Manabe, and Ron Stouffer for sharing their results with us, and to Kirk Bryan for his hospitality during our recent visit to GFDL. This work forms part of the Canadian university participation in the World Ocean Circulation Experiment and is supported by the Natural Sciences and Engineering Research Council of Canada through their Collaborative Research Initiative Programme. Support from the Atmospheric Environment Service through an AES/NSERC Science Subvention Award to RJG is also acknowledged.

REFERENCES

Bjerknes, J., 1964: Atlantic air–sea interaction. *Adv. Geophys.*, **10**, 1–82.

Bryan, K., and M. D. Cox, 1972: An approximate equation of state for numerical models of the ocean circulation. *J. Phys. Oceanogr.*, **2**, 510–514.

——, and R. J. Stouffer, 1991: A note on Bjerknes' hypothesis for North Atlantic variability. *J. Mar. Res.*, **1**, 229–241.

Cai, W., R. J. Greatbatch, and S. Zhang, 1994: Interdecadal variability in an ocean model driven by a small zonal redistribution of the surface buoyancy flux. *J. Phys. Oceanogr.*, in press.

Delworth, T., S. Manabe, and R. J. Stouffer, 1993: Interdecadal variations of the thermohaline circulation in a coupled ocean–atmosphere model. *J. Climate,* **6,** 1993–2011.

Deser, C., and M. L. Blackmon, 1993: Surface climate variations over the North Atlantic Ocean during winter: 1900–1989. *J. Climate,* **6,** 1743–1753.

Dickson, R. R., J. Meinke, S.-A. Malmberg, and A. J. Lee, 1988: The great salinity anomaly in the northern North Atlantic, 1968–1982. *Prog. Oceanogr.,* **20,** 103–151.

Ghil, M., and R. Vautard, 1991: Interdecadal oscillations and the warming trend in global temperature time series. *Nature,* **350,** 324–327.

Gordon, A. L., S. E. Zebiak, and K. Bryan, 1992: Climate variability and the Atlantic Ocean. *EOS,* **73**(15), 161–165.

Greatbatch, R. J., and J. Xu, 1993: On the transport of volume and heat through sections across the North Atlantic: Climatology and the pentads 1955–59, 1970–74. *J. Geophys. Res.,* **98**(C6), 10 125–10 143.

——, A. F. Fanning, A. G. Goulding, and S. Levitus, 1991: A diagnosis of interpentadal circulation changes in the North Atlantic. *J. Geophys. Res.,* **96**(C12), 22 009–22 023.

Hogg, N. G., R. S. Pickart, R. M. Hendry, and W. J. Smethie, Jr., 1986: The northern recirculation gyre of the Gulf Stream. *Deep-Sea Res.,* **33**(9), 1139–1165.

Huang, R. X., 1993: Real freshwater flux as a natural boundary condition for the salinity balance and thermohaline circulation forced by evaporation and precipitation. *J. Phys. Oceanogr.,* **23**(11), 2428–2446.

——, and L. Chou, 1994: Parameter sensitivity study of the saline circulation. *Climate Dyn.,* **9,** 391–409.

Killworth, P. D., 1985: A two-level wind and buoyancy driven thermocline model. *J. Phys. Oceanogr.,* **15,** 1414–1432.

Kushnir, Y., 1994: Interdecadal variations in North Atlantic sea surface temperature and associated atmospheric conditions. *J. Climate,* **7,** 141–157.

Lazier, J. R. N., 1980: Oceanographic conditions at Ocean Weather Ship *Bravo,* 1964–1974. *Atmos.–Ocean,* **18,** 227–238.

Levitus, S., 1989a: Interpentadal variability of temperature and salinity at intermediate depths of the North Atlantic Ocean, 1970–1974 versus 1955–1959. *J. Geophys. Res.,* **94**(C5), 6091–6131.

——, 1989b: Interpentadal variability of salinity in the upper 150m of the North Atlantic Ocean, 1970–1974 versus 1955–1959. *J. Geophys. Res.,* **94**(C7), 9679–9685.

——, 1989c: Interpentadal variability of temperature and salinity in the deep North Atlantic, 1970–1974 versus 1955–1959. *J. Geophys. Res.,* **94**(C11), 16 125–16 131.

Marotzke, J., 1990: Instabilities and multiple equilibria of the thermohaline circulation. Ph.D. dissertation, Ber. Inst. Meeresk. Kiel, 126 pp.

——, 1991: Influence of convective adjustment of the stability of the thermohaline circulation. *J. Phys. Oceanogr.,* **21,** 903–907.

Read, J. F., and W. J. Gould, 1992: Cooling and freshening of the subpolar North Atlantic Ocean since the 1960's. *Nature,* **360,** 55–57.

Roemmich, D., 1989: Sea level and the thermal variability of the ocean. *Sea Level Change: Studies in Geophysics,* National Academy Press, 208–217.

Sato, O. T., and T. Rossby, 1993: Seasonal and secular variations in dynamic height anomaly and transport of the Gulf Stream. Graduate School of Oceanography, University of Rhode Island, Kingston, RI.

Schopf, P. S., 1983: On equatorial waves and El Nino. II: Effects of air–sea thermal coupling. *J. Phys. Oceanogr.,* **13,** 1878–1893.

Weaver, A. J., and E. S. Sarachik, 1991a: The role of mixed boundary conditions in numerical models of the ocean's climate. *J. Phys. Oceanogr.,* **21,** 1470–1493.

——, and ——, 1991b: Evidence for decadal variability in an ocean general circulation model: An advective mechanism. *Atmos.–Ocean,* **29**(2), 197–231.

——, J. Marotzke, P. F. Cummins, and E. S. Sarachik, 1993: Stability and variability of the thermohaline circulation. *J. Phys. Oceanogr.,* **23,** 39–60.

——, S. M. Aura, and P. G. Myers, 1994: Interdecadal variability in an idealised model of the North Atlantic. *J. Geophys. Res.,* in press.

Winton, M., and E. S. Sarachik, 1993: Thermohaline oscillations induced by strong steady salinity forcing of ocean general circulation models. *J. Phys. Oceanogr.,* **23,** 1389–1410.

Yang, J., and J. D. Neelin, 1993: Sea-ice interactions with the thermohaline circulation. *Geophys. Res. Lett.,* in press.

Zhang, S., C. A. Lin, and R. J. Greatbatch, 1992: A thermocline model for ocean climate studies. *J. Mar. Res.,* **50**(1), 99–124.

——, R. J. Greatbatch, and C. A. Lin, 1993: A reexamination of the polar halocline catastrophe and implications for coupled ocean–atmosphere models. *J. Phys. Oceanogr.,* **23,** 287–299.

——, C. A. Lin, and R. J. Greatbatch, 1994: A decadal oscillation due to the coupling between an ocean circulation model and a thermodynamic sea-ice model. *J. Mar. Res.,* in press.